1

INTRODUCTION

Ferroelectricity was discovered in 1921 by Joseph Valashek [1]. Ferroelectricity is a phenomenon of developing a spontaneous electric polarization in certain materials, mostly dielectrics. The spontaneous electric polarization can be reversed in direction by the application of the electric field. The effect resembles a more familiar magnetic polarization in ferromagnets. By this analogy the materials were baptized “ferroelectrics” in spite of the fact that most of them do not content iron at all [2].

In Ferroelectric materials the polarization is not determined by the applied field E alone but depends upon the previous history of the material. If a virgin specimen (not subject to an electric field previously) of a ferroelectric material subjected to an electric field, the field is gradually increased[3], and then decreased through zero ,then the curve trace out between P-E is known as Hysteresis loop for ferroelectric materials. The spontaneous polarization of ferroelectric materials implies a hysteresis effect which can be used as a memory function, and ferroelectric capacitors are indeed used to make ferroelectric RAM [11].

Ferroelectric thin films have received considerable attention because of their use in non-volatile memory applications (FRAMs)[4,5]. Main applications of ferroelectric materials are in: capacitor, non volatile memory, Piezoelectrics for ultrasound imaging and actuators, electro optic application for data storage application, Thermistors , Switches known as transchargers or transpolarizers, Oscillators and filters, Light deflectors, modulators and displays[6] .

1.1. Dielectrics:

These materials provide electrical insulation between two media which are at different potential and also act as stores of electrical charges (in capacitors). When main

function is insulation, the materials are called as insulating materials, and when charge store is the main function they are termed as Dielectrics [3].

In these materials the electron are bound so tightly to their respective atomic nuclei that electrical conduction by electrons cannot occur. These materials show their effect under the influence of an electric field, and they give rise to new phenomenon called polarization, which helps in storing electrostatic energy (in dielectric). Under the influence of an alternating field, their behaviour can be understood by complex dielectric constant [3].

1.1.1. General properties of dielectrics:

1.1.1.1. Dielectric Polarization:

In dielectric materials, all electrons are bound; the only motion possible in the presence of an electric field is a minute displacement of positive and negative charges in opposite directions.

The displacement is usually small compared to atomic dimensions. A dielectric in which this charge displacement take place is said to be polarized, and its molecules are said to be posses induced dipole moments. These dipoles produce their own field, which adds to that of external field [3].

In addition to displacing the positive and negative charges, an applied electric field can also polarize a dielectric by orienting molecules that posses a permanent dipole moment. Such molecules experience a torque which tends to align them with the field but collisions arising from the thermal agitation of the molecules tend to destroy the alignment. An

equilibrium polarization is thus established in which there is, on the average a net alignment [3].

The magnitude of polarization P of dielectric materials numerically describes the phenomenon of polarization of a dielectric in an external electric field. The action of an external electric field forces the molecules of the dielectric in to a certain ordered arrangement in space. The polarization P can be expressed quantitatively as the sum of the electric dipole moment per unit volume V,

$$P = \frac{\sum p}{v} \tag{1.1}$$

Compared to air filled capacitors, dielectric capacitors can store more electric charge due to the dielectric polarization P. The physical quantity called the electric displacement D is related to electric field E by following expressions [7]:

$$D = \varepsilon_o + P \tag{1.2}$$

The relation between P and E for isotropic materials is:

$$P = \varepsilon_o (\varepsilon_r - 1) = \chi_e \varepsilon_o E \tag{1.3}$$

Where ε_o denotes the permittivity of free space = 8.854×10^{-12} F/m and the constant of proportionality ε_r being defined as the relative dielectric constant and χ_e is dielectric susceptibility.

(1) Electronic polarization:

Electronic polarizaiton occurs in all dielectric materials. This type of polarization has been explained with the help of rare gas atoms, in which it is assumed that the interaction among the atoms is negligible. This is because the distance between the molecules is large enough and any neighbour – neighbour reactions can be eliminated. A simple model of an

atom having a positive nucleus of charge surrounded by a spherical negative charge. It is assumed that the charge cloud is of uniform density, with no external field, the nucleus is at the centre of this sphere of charge. Under influence of the field E, the nucleus and electron cloud shift with respect to one another by some distance [3], this effect will induce a dipole moment. The strength of the induced dipole moment $\mu_{e,}$ for an atom is proportional to the local field in the region of the atom and is given by the equation where α_e is:

$$\mu_e = \alpha_e E_{ioc} \tag{1.4}$$

called the electronic polarizability; it is sometimes also referred to as the optical polarizabilty. E_{ioc} is subjected to homogenous electric filed. Electronic polarization can follow alternating fields with frequency up to THz – PHz (10^{12} – 10^{15} cycle/second, higher than visible light wave) [8].

(2) Ionic polarization:

Ionic polarization exits only for those types of materials which have a net positive charge. Even in the absence of electric field, HCL molecule has a permanent dipole moment q.d; where d is the distance of separation of ions, q is the charge on the molecule. In an electric field the resultant torque lines up the dipoles parallel to the field at absolute zero of temperature. The field has induced an additional dipole moment, this induced dipole moment is proportional to the applied electric field, and the proportionality constant, $\alpha_{i\ ,}$ is the ionic polarizability [3].

$$P_{ind} = \alpha_i \mathbf{E} \tag{1.5}$$

Distribution of electrons in both atoms and molecules is almost completely independent of temperature, so both electronic and ionic polarizibilities are independent of temperature [3].

(3) Orientation/dipolar polarization:

Dipolar polarization involves reorientation of permanent dipoles. This polarization occurs generally in liquids and solids which have asymmetric with permanent dipole moments. A permanent dipole moment is caused by unbalanced sharing of electrons by atoms of a molecule. In an absence of an external electric field, these moments are oriented in a random order such that no net polarization is present. Under an external electric field, the dipoles rotate to align with the electric field causing orientation polarization to occur [13].

The dipole reorientation can follow up to frequency (10^9 cycle/ sec). The frequency dependence of orientation polarization α_d, can be expressed as [9]:

$$\alpha_d = \frac{\alpha_{do}}{1 + j\omega\tau} \tag{1.6}$$

Where α_{do} is the low frequency polarizabilty and τ is the time constant involved in the reoriention process, ω is field's frequency.

(4) Space Charge Polarization:

Free charge carriers, migrating through the crystal under the influence of an electric filed may be trapped by, pile up against defect, such as lattice vacancies, impurity centres, dislocations, and so on. The effect of this will be the creation of a localized accumulation of charges which will be induce its image charges on an electrode and give rise to dipole moments. This constitute a separate mechanism in dielectrics, called Space charge polarization [3].. The relaxation frequencies can be as low as Hz – 1 KHz [11,12]. Any or all

of the above mechanism may be contributing to the observed behaviour in an applied electric field. Thus, polarizabilty is the sum of individual polarizibilities, each arising from one particular mechanism and is expressed by the equation

$$\alpha = \alpha_e + \alpha_i + \alpha_d + \alpha_s \quad (1.7)$$

Where α represents the total polarizability of the respective polarization mechanisms; electronic (α_e), ionic (α_i), dipolar (α_d), and space charge polarization (α_s).

1.1.1.2. Dielectric constant and dielectric loss:

(1) Dielectric constant:

The relative permittivity of a material under given conditions reflects the extent to which it concentrates electrostatic lines of flux. In technical terms, it is the ratio of the amount of electrical energy stored in a material by an applied voltage, relative to that stored in a vacuum. Likewise, it is also the ratio of the capacitance of a capacitor using that material as a dielectric, compared to a similar capacitor that has a vacuum as its dielectric [14].

If the medium to which the field is applied is free space (vacuum), it is known as dielectric constant of vacuum, ε_o of value $8.854*10^{-12}$ farad/meter, the dielectric constant of a material may be expressed by ε_r, relative to vacuum by: [3].

$$\varepsilon_r = \frac{\varepsilon}{\varepsilon_o} \quad (1.8)$$

ε is the permittivity of the medium in which the charge is placed, its unit is farad/meter. If dc voltage *V* is applied across a parallel plate capacitor (fig 1.1) .A dielectric slab is placed between the plates of a parallel plate capacitor. The dielectric material increases the storage

capacity of the capacitor. The capacitance with the dielectric material is related to the dielectric constant as indicated in the following equation [3,8]:

$$C_o = \frac{A}{d}\varepsilon_o \tag{1.9}$$

$$C = C_o\, \varepsilon_r \tag{1.10}$$

Where C , C_o are capacitance with and without dielectric, ε_r is the permittivity of the dielectric medium, and A and d are the area of the capacitor plates and the distance between them, respectively

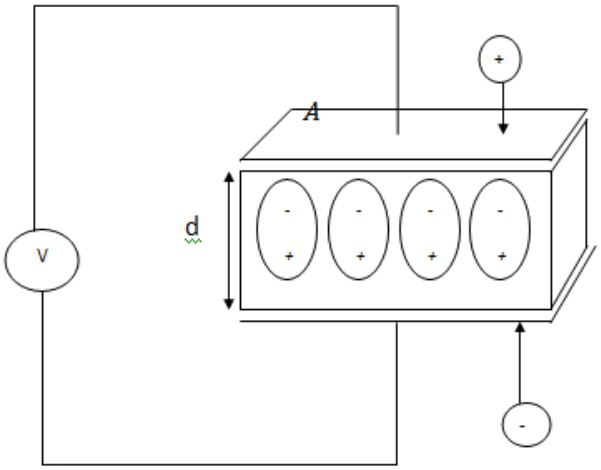

Fig. 1.1 : Parallel plate capacitor under DC field

When an alternating e.m.f. is applied across the capacitor plates, an alternating current will flow; its value being:

$$i = j\omega C_o\, \varepsilon_r v \tag{1.11}$$

Where ε_r is relative permittivity of dielectric, ω is frequency of applied signal, Co is capacitance in vacuum, v is the applied ac voltage. In general, however, an inphase component of current will appear corresponding to a resistive current between the capacitor plates. Such current is entirely due to dielectric medium and is a property of it. Therefore, the permittivity is characterized by a complex quantity [3]:

$$\varepsilon_r = \varepsilon_r' - j\varepsilon_r'' \tag{1.12}$$

Dielectric constant / relative permittivity (ε_r) is equivalent to absolute permittivity (ε) relative to the permittivity of free space (ε_o). The imaginary part of permittivity (ε''_r) is always greater than zero and is usually much smaller than (ε'_r), the current in the capacitor then becomes :

$$i = j\omega(\varepsilon_r' - j\varepsilon_r'')C_o v \tag{1.13}$$

$$i = \omega\varepsilon_r'' C_o v + j\omega\varepsilon_r' v C_o \tag{1.14}$$

and this has a real component, which is a loss component of current.

(2) Dielectric loss:

Where an ac voltage is applied to a dielectric between two electrodes the dielectric is subjected to alternating field (stress). The alternating of this stress involves molecular arrangement with in dielectric. This involves energy loss with each reversal. This is because the molecules have to overcome a certain amount of internal friction in the process of alignment. The energy explained in the process is released as heat in the dielectric. This is called dielectric loss. The dielectric loss is not applicable at 50 Hz but at higher frequency in megahertz range it because appreciable for some dielectrics. Special dielectric materials are

available (like special plastic, ceramics, glass etc.) which have low loss at higher frequencies [3].

It has been seen earlier that electronic, ionic, and orienational polarization lead to a complex dielectric constant when a dielectric is subjected to an alternating field, the dielectric constant which has real and imaginary parts is expressed as:

$$\varepsilon_r = \varepsilon_r' - j\varepsilon_r'' \tag{1.15}$$

Where ε''_r imaginary part of permittivity and ε_r' is real part of permittivity. It is customary to characterize the dielectric losses at a certain frequency and temperature by a factor called **loss tangent, tanδ** , defined as:

$$\tan\delta = \frac{\varepsilon_r''}{\varepsilon_r'} \tag{1.16}$$

When complex permittivity is drawn as a simple vector diagram, the real and imaginary components are 90^o out of phase.

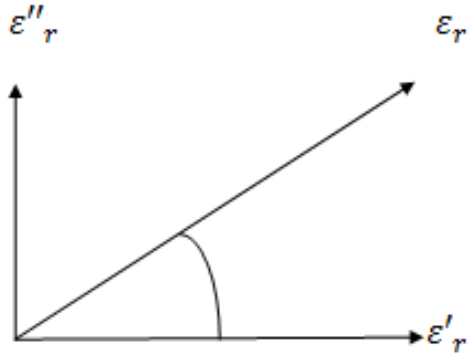

Fig 1.2: Loss tangent vector diagram

1.2. Ferroelectricity:

The phenomenon of reversal of direction of the spontaneous polarization by the application of strong enough E is known as ferroelectricity [9]. The ferroelectric properties of ferroelectric materials disappear above a critical temperature T_c; this phase temperature is called the ferroelectric curie temperature [15]. The phase transition from the ferroelectric to the paraelectric phase is associated with anomalies in the physical properties like specific heat, dielectric constant, spontaneous polarization, etc.

1.2.1. General properties of ferroelectrics

1.2.1.1. Crystal Symmetry:

Structural symmetry of a crystal depends on its lattice structure. The lattice structure is described by Bravais unit cell of the crystal [16]. Though there are thousands of crystals in nature, they all can be grouped together into 230 microscopic symmetry types or space groups based on the symmetry elements [17]. Structural symmetry of a crystal affects geometrically both structural and physical properties of the crystal, such as dielectric, elastic, piezoelectric, ferroelectric and non linear optical properties, etc [16].

1.2.1.2. Spontaneous polarizarion and Pyroelectric effect:

The spontaneous polarization is given by the value of the dipole moment per unit volume or by the value of the charge per unit area on the surface perpendicular to the axis of spontaneous polarization. Since electrical properties are strongly correlated with the crystal axis, the axis of spontaneous polarization is usually a crystal axis [16].

Although a crystal with polar axes exhibits piezeoelectric effect, it does not necessarily have a spontaneous polarization vector, because the net result of electric moments

along all polar axis may be equal to zero. Therefore, only a crystal with unique polar axis exhibits a spontaneous polarization. In general, this spontaneous polarization cannot directly be measured from the charges are compensated by external and /or internal carriers carrying an electric current, or by charges on the boundaries of twins. The value of spontaneous polarization depends on temperature [16]. . If the temperature of crystal is altered, a change in polarization occurs and electric charges can be observed on those crystal faces. This is the pyroelectric effect, a pyroelectric material is one which exhibits a spontaneous polarization in the absence of electric field and changes its polarization on heating, All crystal that shows ferroelectric behaviour is pyroelectric, but not vice versa [3,18].

1.2.1.3. Ferroelectric Domains:

As described above, pyroelectric crystals show a spontaneous polarization $\mathbf{P_s}$ in a certain temperature range. If the magnitude and direction of $\mathbf{P_s}$ can be reversed by an external electric field, then such crystals are said to show ferroelectric behaviour. From a physical point of view, ferroelectric crystal are those crystal which posses one or more ferroelectric phases. The ferroelectric phase in particular state exhibiting spontaneous polarization which can be reoriented by an external field. A reversal of polarization is considered as a special case of polarization reorientation [16].

In general, uniform alignment of electric dipoles only occurs in certain region of crystal, while in other region of crystal spontaneous polarization may be in the reverse direction. Such region with uniform polarization are called ferroelectric domain. The interface between two domains are called the domain wall [16].

1.2.1.4. Hysteresis Loop:

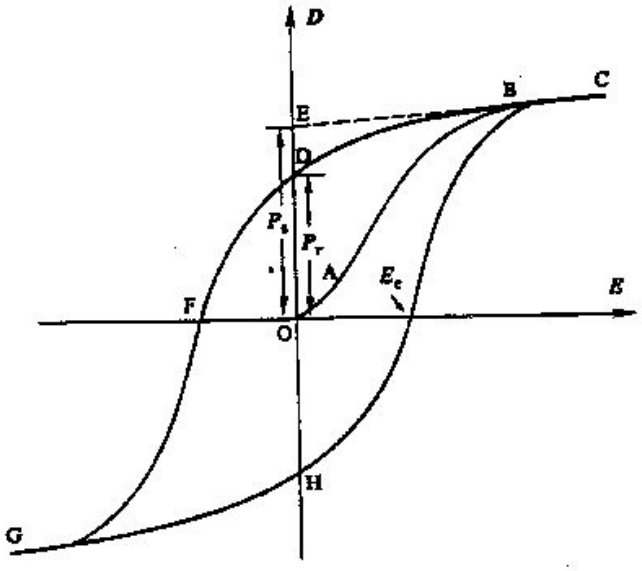

Fig 1.3*:* A Polarization vs. Electric Field (P-E) hysteresis loop for a typical ferroelectric crystal. [19]

Ferroelectric materials, in which polarization is the unique function of the field. Ferroelectric materials exhibits hysteresis loop analogous to ferromagnetic materials. In these materials the polarization is not determined by the applied field E alone but depends on the previous history of the material. If a specimen (not subjected to an electric field previously) of a ferroelectric is subjected to an electric field, and the field is gradually increased, the polarization P increases along the curve OABC. When the field is then gradually decreased, it is found that If E=0, there is a polarization still left. This Polarization is called as the remnant polarization, P_r .In the other words, the materials is spontaneously polarized. An electric field Ec is required to reduce the polarization to zero. Ec is called as the coercive field and has to be applied in opposition direction. The existence of a dielectric hysteresis loop in the material implies that the substance possesses spontaneous polarization, i.e. polarization that persists when applied field is zero [3].

1.2.1.5. Curie temperature and phase transition:

Another important characteristic of ferroelectric materials is the temperature of phase transition called Curie temperature. When temperature decreases through the curie point, a ferroelectric crystal undergoes a structural phase transition from a paraelectric phase to ferroelectric phase. When the temperature is above the curie point the crystal does not exhibit ferroelectricity. It is generally believed that the ferroelectric structure of a crystal is created by a small distortion of the paraelectric structure such that the lattice symmetry in the ferroelectric phase is always lower than that in paraelectric phase [16].

In some ferroelectrics, a simple law, called the curie – Weiss law, can describe the temperature dependence of the dielectric constant above the transition temperature fairly accurately:

$$\varepsilon = \varepsilon_o + \frac{C}{T - T_o} \qquad (1.17)$$

Where the temperature- independent part ε_o can often be neglected, C is the curie constant and T_0 the curie – Weiss temperature [3,12] .

1.2.2. Application of ferroelectric materials:

Applications of ferroelectric materials utilize their unique properties, like dielectric, piezoelectric, pyroelectric, and electro-optic properties. In the following section, application have been discussed on the basis of the properties.

(1) Ferroelectric memories:

The spontaneous polarization of ferroelectric materials implies a hysteresis effect which can be used as a memory function, and ferroelectric capacitors are indeed used to make ferroelectric_memories [11].

One of the problems with ferroelectric memories is the tendency to lose its ability to store data after a certain number of read/ write cycles, this phenomenon is called fatigue. To avoid this problem, now a days SBT is using in ferroelectric memories as a ferroelectric material due to their anti fatigue properties.

(2) Capacitor:

Ferroelectric can be used to make capacitors (usually pervoskite). Their value of dielectric constant can be changed depending on changes in the magnitude and direction of electric field. Under these condition they can be behave like a varactors. Such capacitor may be also used as radio frequency power amplifier. In this application electric field changes the dielectric constant and thus, in turn changes the power supply [3].

(3) Electro-optic Applications:

The requirements for using ferroelectric thin films for electro-optic applications include an optically transparent film with a high degree of crystallinity. A great deal of work has been done on making ferroelectric thin film waveguides from $LiNbO_3$ and $Li(Nb,Ta)O_3$. PZT and PLZT thin films are even better candidates for optical waveguide applications because of their large electro-optic coefficients [20-22].

(4) Pyroelectric devices:

Pyroelectricity is utilized in the fabrication of pyrodetectors like temperature / infrared light sensors and infrared image sensors. Pyroelectric detectors are thermal detectors. That is, they produce a signal in response to a change in their temperature. Below a temperature Tc known as the Curie point, ferroelectric materials, exhibit a large spontaneous electrical polarisation. If the temperature of such a material is altered, for example, by incident radiation, the polarisation changes [23].

(5) Piezoelectric Devices:

Piezeoelectric crystal is used in numerous devices, such as High voltage and power sources, Sensors, Actuators, Frequency standard, Piezoelectric motors, Surgery and so on.

1.2.3. Type of Ferroelectric materials:

There are four main type of ferroelectric materials according to their structure.

(1) Perovskites:

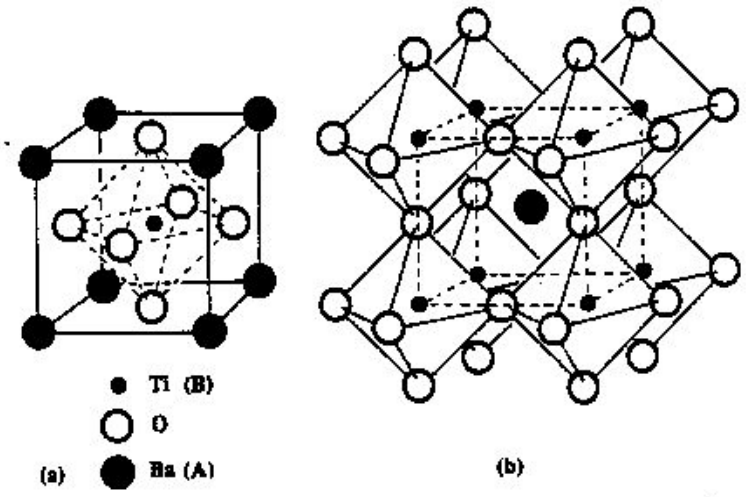

Fig 1.4 :(Peroskites structure),(a) A cubic ABO_3 ($BaTiO_3$) perovskite-type unit cell and (b) three dimensional network of corner sharing octahedra of O^{2-} ions[14]

Perovskite is a family name of a group of materials and the mineral name of calcium titanate ($CaTiO_3$). Many piezoelectric (including ferroelectric) ceramics such as Barium Titanate ($BaTiO_3$), Lead Titanate ($PbTiO_3$), Lead Zirconate Titanate (PZT), Lead Lanthanum Zirconate Titanate (PLZT), Lead Magnesium Niobate (PMN), Potassium Niobate ($KNbO_3$), Potassium Sodium Niobate ($K_xNa_{1-x}NbO_3$), and Potassium Tantalate Niobate ($K(Ta_xNb_{1-x})O_3$) have a perovskite type structure. These oxide ceramics have the general formula ABO_3 [14]. A represents a cation with a larger ionic radius while B represent a cation with smaller ionic radius. Figure 1.4(a) shows a cubic ABO_3 . e.g. A is Ba and B is Ti in $BaTiO_3$ [16].

A perovskite structure is essentially a three dimensional network of BO_6^- octahedral as shown in fig 1.4(b): it may be regard as a cubic close packed arrangement of A and O ions with B ions filling the octahedral interstitial position [16].

(2)Tungsten Bronze type Compounds:

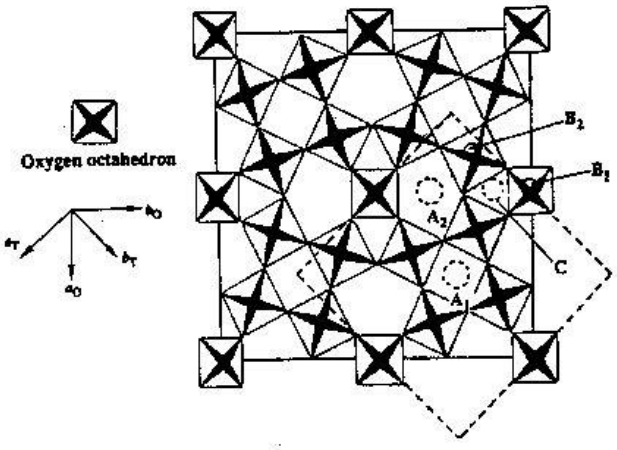

Fig:1.5 Schematic diagram showing a projection of the tungsten-bronze structure on the (001) plane. The orthorhombic and tetragonal cells are shown by solid and dotted lines respectively[16].

There are many tungsten bronze type ferroelectric crystal. The tungsten bronze type ferroelectric crystals have a structure similar to tetragonal tungsten bronze K_xWO_3 ($x<1$). Lead niobate ($PbNb_2O_6$) was one of the first crystals of the tungsten bronze type structure to show useful ferroelectric properties. The oxygen octahedral frame work of TB type niboate is shown in fig 1.5, there are three type of sites A_1,A_2 and C. The central site of the oxygen octahedron is also of two type B_1, B_2, each having different symmetry positions. A tetragonal unit cell includes two A1 sites four A2 sites ,Four C site two B1 site , eight B2 site and thirty oxygen ions (at the corners of the octahedral).The site occupancy formula for this type of structure is given by $(A_1)_2(A_2)_4(C)_4(B_1)_2(B_2)_8O_{30}$. For lead niobate the B_1 and B_2 sites are occupied by Nb^{5+} ions or Ta^{5+} ions. While A_1, A_2 and C sites are occupied by either alkaline earth ionsor alkali ions or both.[16] .

(3) Bismuth Oxide Layer Structured Ferroelectrics:

These ferroelectric do not have oxygen-octahedra structure. With the exception of the bismuth layer structured ferroelectric family. These crystals have rather unique properties especially their variable optical anisotropic properties make them extremely attractive in applications such as memory and display devices etc [16]. The two most important piezoelectric materials with the $(Bi_2O_2)^{2+}$ layer structure are bismuth titanate ($Bi_4Ti_3O_{12}$) and lead bismuth niobate ($PbBi_2Nb_2O_9$). The plate like crystal structure of these compounds leads to highly anisotropic ferroelectric properties [16].

(4) Lithium Niobate and Tantalate:

Lithium niobate ($LiNbO_3$) and lithium tantalate ($LiTaO_3$) have similar structures. In view of their excellent piezoelectric, pyroelectric, and optical properties. They are well

known ferroelectric crystals and have been extensively studies for various device applications. Ferroelectricity in these crystal was discovered in 1949 [16].

Currently many devices such as high frequency and high temperature tranducers, infrared detectors, laser modulator, laser frequency multiplier, optical parameter oscillator, optical wave guide etc, are made with Lithium niobate ($LiNbO_3$) and lithium tantalate ($LiTaO_3$), These crystals are very stable with very high Curie points of 1240° C for $LiNbO_3$[16].

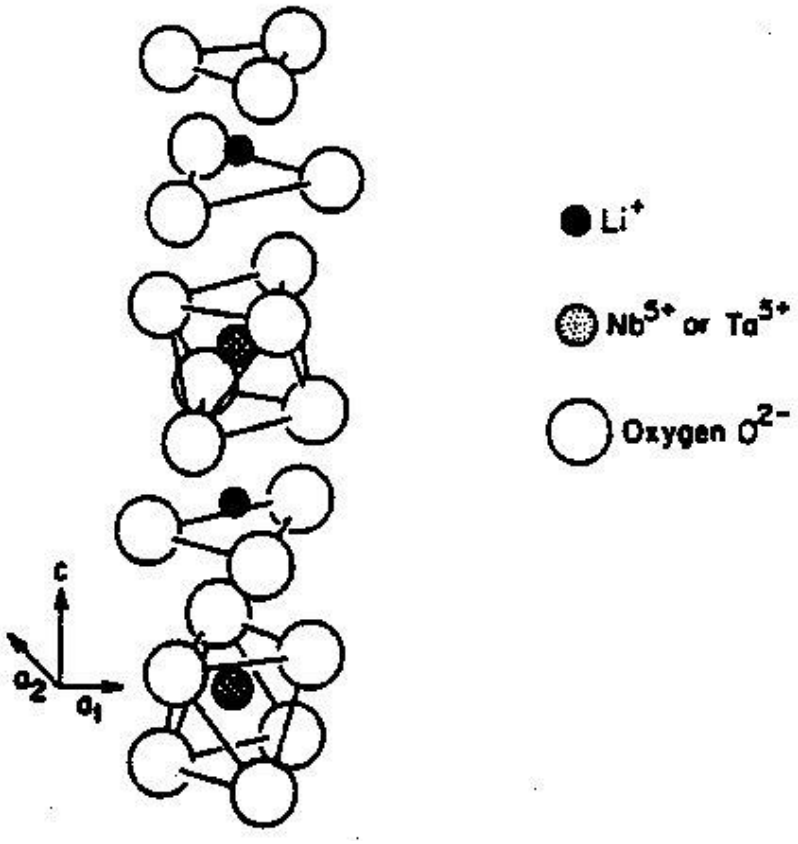

Fig. 1.6 : Structure of Ferroelectric $LiNbO_3$ and $LiTaO_3$ [24]

The structure for both $LiNbO_3$ and $LiTaO_3$ are shown in fig 1.6, the crystal structure of ABO_3 is composed of oxygen octahedral and the neighbouring oxygen octahedra are connected to each other through an oxygen ion [16].

1.3. Strontium bismuth tanatalate, $SrBi_2Ta_2O_9$:

Lead zirconate titanate (PZT) has attracted a great deal of attention for use in non-volatile memory and microelectromechanical system (MEMS) applications due to its large remnant polarization (Pr) and small coercive field (Ec) [25]. However,PZT films with Pt electrodes suffer from fatigue in which the remnant polarization declines after about 10^8 switching cycles. Recently, bi-layered perovskite ferroelectric films such as strontium bismuth tantalate ($SrBi2Ta_2O_9$, SBT) have become attractive candidates due to their low leakage current, minimal tendency to imprint, and, in particular, the small amount of fatigue with platinum electrodes [26]. It exhibits Almost no fatigue after 10^{12} cycle, good retention characteristics [5]. SBT belongs to the Aurivillius family of bismuth oxide layered structures [29].

The chemical formula of this family is given by:

$$(Bi_2O_2)^{2+}(A_{m-1}B_mO_{3m+1})^{2-},$$

Where A and B represent the ions with suitable chemical valances and ionic radii. Usually A represents Pb, Ba, Sr, Ca, Na, K, and rare earth elements, B represents Ti,Nb,Ta,W,Mo,Fe,Co,Cr etc [14]. m denoted the number of octahedral layers with in pervoskite sublattice of the structure and (m=1,2,…..5)[16,5].

It is well known that the Aurivillius composition **$SrBi_2Ta_2O_9$** (SBT) is a bismuth layered pseudo pervoskite oxide with m=2 and show ferroelectric behaviour at room temperature [27,28]. In the SBT crystal, pseudo-perovskite blocks, $(SrTa_2O_7)^{2-}$, composed of double TaO_6 octahedra with Sr at the A-site are interleaved with $(Bi_2O_2)^{2+}$ layers [30,5], strontium bismuthetantalate $SrBi_2Ta_2O_9$ (SBT) have a (pseudo) tetragonal perovskite

structure[29]. Bismuth layer is responsible for determining the ferroelectric and electrical properties of these ceramic [31] Nature of bismuth layer is paraelectric while structures of perovskite unit cell are ferroelectric [31,32].

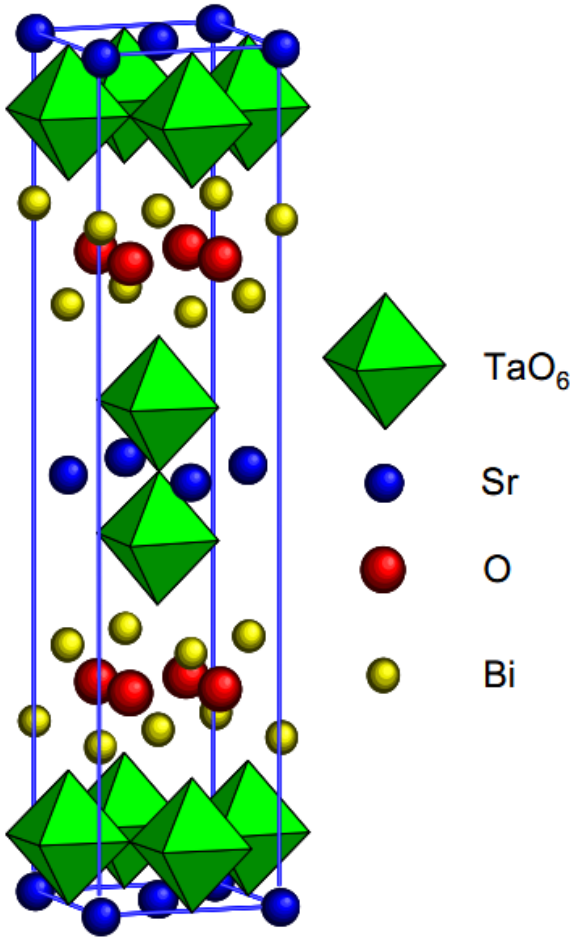

Fig 1.7: Bismuth layered oxide SBT structure

2

EXPERIMENTAL TECHNIQUES

2.1. Composition Prepared:

Strontium Bismuth Tantalate ($SrBi_2Ta_2O_9$):

The starting chemical used were strontium carbonate ($SrCo_3$), Bismuth oxide (Bi_2O_2) and Tantalum oxide (Ta_2O_5). All the chemical acquired were from Aldrich chemical company, USA.

2.2. Experimental Procedure:

2.2.1. Solid state reactions method:

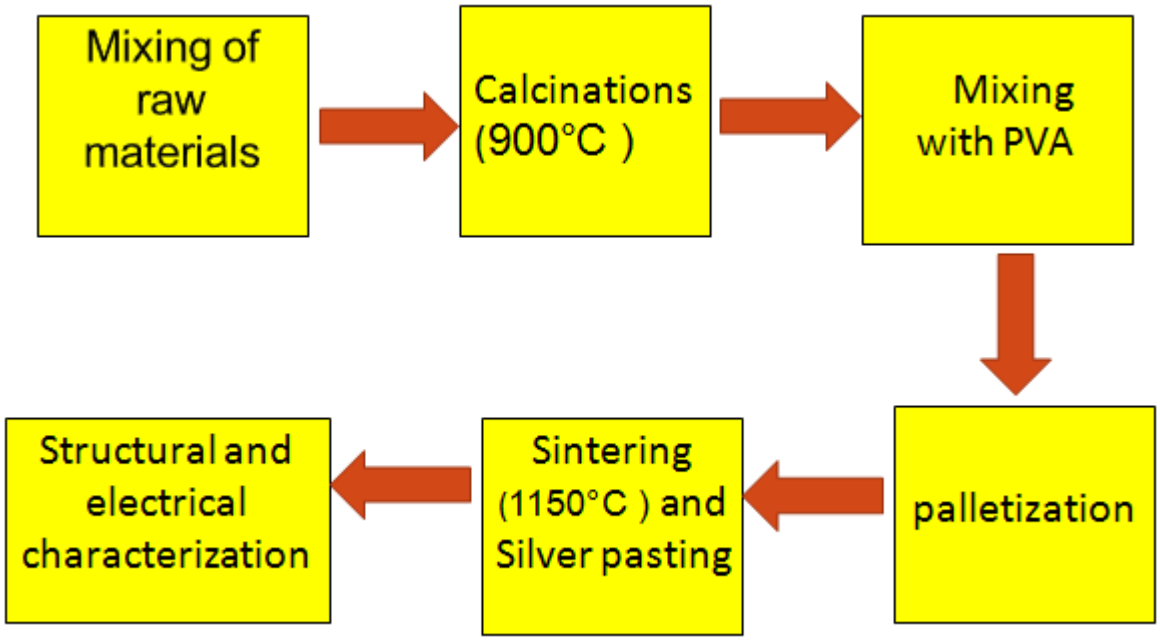

Fig; 2.1: Block diagram of Solid State Reaction Technique

The high purity raw materials (oxides and carbonates) are first weighed according to the stoichiometric formula of the composition. The particle size of the powders must be in the submicron range for the solid phase reactions to occur by atomic diffusion. The next step is mixing, eliminating aggregates and /or reducing the particle size by thoroughly grinding the

mixture. Calcination Process helps in the decomposition of the constituent carbonates resulting in the formation of oxides and removal of the carbon dioxide. For example,

$$SrCo_3 \longrightarrow SrO + CO_2\uparrow$$

During the calcinations step, the solid phase reaction takes place between the constituents giving the partial/ complete ferroelectric phase. Calcination causes the constituents to interact by interdiffusion of their ions.

After calcinations, lumps are crushed and grinded it is necessary to add an organic binder like Polyvinyl Alcohol (PVA) for sufficient adhesion during pelletization. After shaping the compactive powder in to pellet it sinter at high temperature to form a denser structure of crystallite join to one another by grain boundary. The sintered pellets are polished by silver paste to provide electrical contact.

2.2.2. Mechanical Activation Techniques:

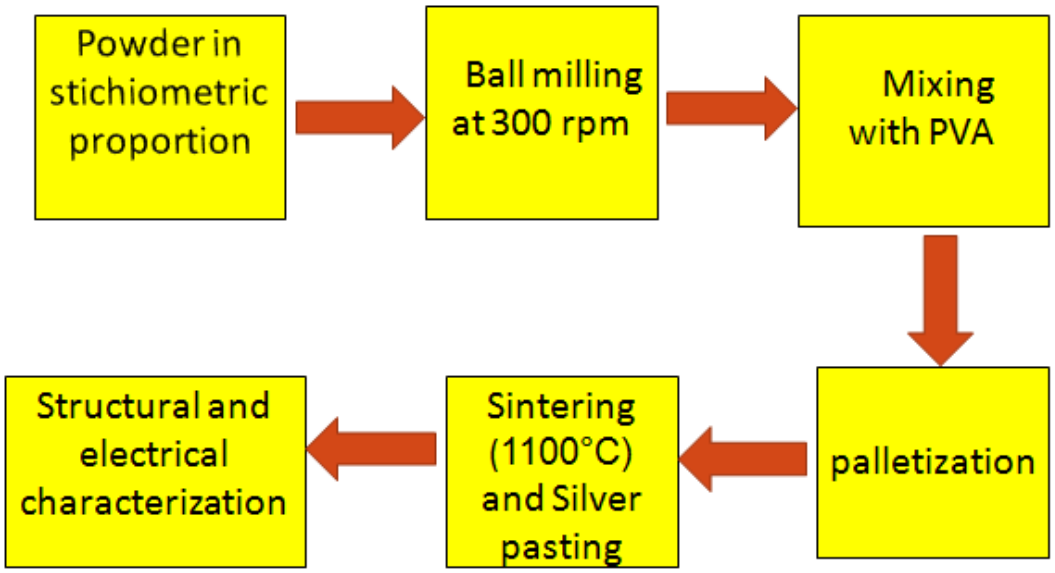

Fig; 2.2 : Block Diagram of Mechanical Activation Technique

In this technique the formation of the desired compound is due to the reaction of the oxide which is activated by mechanical energy, instead of heat energy required in the conventional solid state reaction method. Highly pure powders of $SrCO_3$, Bi_2O_3, Ta_2O_5 (all from M/s Aldrich) were mixed to yield $SrBi_2Ta_2O_9$. This mixture of powders was milled in a high-energy planetary ball mill (Retsch, PM 100) for 5, 10, 20 hrs at a milling speed of 300rpm. Milling was carried out in toluene medium with a high wear-resistant 10mm zirconium oxide balls in a zirconium oxide vial with a ball-to-powder weight ratio of 10:1. The mixture was then admixed with 2wt% polyvinyl alcohol as a binder and then pressed at 200 MPa into a disk shaped pellet. These pellets were then sintered at 1100°C for 2 hrs in air on alumina crucibles.

2.3. Experimental Techniques used for characterization.

X-ray diffraction technique: used for the phase identification of synthesized specimen.

2.3.1. XRD:

X-ray crystallography is a technique in which the pattern produced by diffraction of X- rays through the closely spaced atoms of crystals is recorded and then analyzed to reveal the nature of the lattice. The spacing in the crystal lattice is determined by the well known Bragg's law [44].

In an X-ray diffraction measurement, a crystal is mounted on a goniometer and gradually rotated while being bombarded with X-rays, producing a diffraction pattern of regularly spaced spots known as reflections [44].

The two-dimensional images taken at different rotations are converted into a three-dimensional model of the density of electrons within the crystal using the mathematical method of Fourier transforms, combined with chemical data known for the sample [44].

The pattern of diffraction peaks can be used to identify the material using JCPDS (Joint committee of powder diffraction standards) pattern database and change in peak width and position can be used to determine crystal size and phases.

Phase identification:

The most widespread use of this technique is the identification of crystalline solid. Each crystalline solid produces its own diffraction pattern. Both the position and the intensity of the lines are characteristics of that particular phase and the pattern thus provides a fingerprint of the material.

2.3.2. Scanning Electron Microscope:

Fig 2.3: Scanning Electron Microscope

The essential parts of SEM are shown in the figure 2.4. In SEM electrons emitted from a hot filament are usually used. In SEM backscattered electrons or secondary electrons are detected (in some cases it is also possible to use sample current). Due to interaction of focused beam with solid, the backscattered electrons are somewhat defocused resulting in to lowered resolution than one would expect [44].

In an electron microscope, the electron beam can be focused to a very small spot size using electrostatic or magnetic lenses. Usually the electromagnetic lenses are used for SEM. The fine beam is scanned or rastered on the sample surface using a scan generator and back scattered electrons are collected by an appropriate detector [44].

Signal from scan generator along with amplified signal from the electron collector generates the image of sample surface. In order to avoid the oxidation and contamination of filament as well as reduce the collision between air molecules and electrons, filament and sample have to be focused in a vacuum chamber. Usually vacuum -10^{-5} torr or better is necessary for a normal operation of SEM. This makes electron microscopes rather inconvenient [44].

One disadvantage of electron microscopes is that insulating samples cannot be analyzed directly as they get charged due to incident electrons and images become blurred/faulty. Therefore insulating solids are coated with a very thin metal film like gold or platinum (<10 nm) making them conducting without altering any essential details of the sample. The metal film is usually sputter coated on the sample to be investigated prior to the introduction in to the electron microscope. This enables even biological sample to be analyzed using an electron microscope [44].

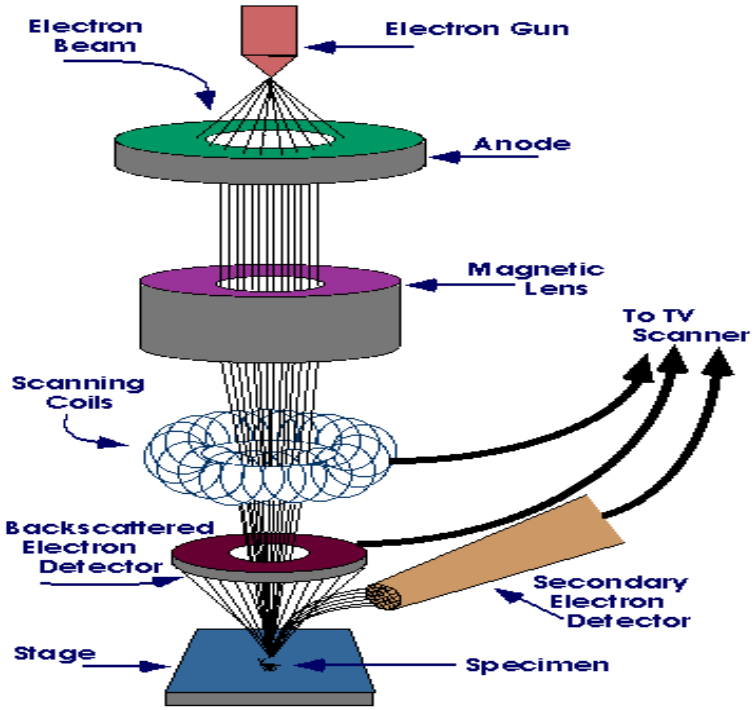

Fig 2.4: Essential Parts of Scanning Electron Microscopy

2.3.3. LCR meter:

A LCR meter (Inductance (L), Capacitance (C), and Resistance (R)) is a piece of electronic test equipment used to measure the inductance, capacitance and, resistance of a component. In the usual versions of this instrument these quantities are not measured directly, but determined from a measurement of impedance. The necessary calculations are, however, incorporated in the instrument's circuitry; the meter reads L, C and R directly with no human calculation required [45].

Usually the device under test (DUT) is subjected to an a.c. voltage source. The meter detects the voltage over, and the current through the DUT. From the ratio of these the meter can determine the magnitude of the impedance. The phase angle between the voltage and

current is also detected and between that and the impedance magnitude the DUT can be represented as an L and R or a C and R. The meter must assume either a parallel or a series model for these two elements. The most useful assumption, and the one usually adopted, is that LR measurements have the elements in series (as would be encountered in an inductor coil) and that CR measurements have the elements in parallel (as would be encountered in measuring a capacitor with a leaky dielectric).It can also be used to judge the inductance variation with respect to the rotor position in permanent magnet machines [45].

Working Principle of LCR Meter:

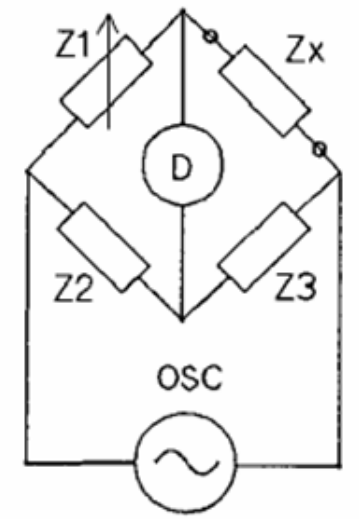

Fig 2.6: Measurement of unknown impedance using LCR Meter

LCR meters for electrical properties measurement at low frequencies are based on Auto balancing bridge method and the one for measurements at high frequencies employ the RF I-V method. In automatic balancing bridge method, the device under test (DUT) is placed in a bridge as shown in Figure 2.6. The DUT impedance is represented by Zx. The impedance Z_2 and Z_3 are known, and Z_1 is changed until no current flows through D i.e. the terminals of D are made equi-potential. Z_{DUT} is then calculated using the equation [46]:

$$Z_{DUT} = (Z_3/Z_2)\, Z_1$$

2.3.5. Ball milling:

It is one of the simplest ways of making nanoparticles of some metals and alloys in the form of powder. There are many types of mills viz. planetary, vibratory, rod, tumbler, etc. Usually one or more containers are used at a time to make fine particle. Size of container, of course, depends upon the quantity of interest. Hardened steel or tungsten carbide (in our experiment zirconium oxide ball is used) balls put in containers along with powder or flakes (<50µm) of a material of interest. Initial materials can be of arbitrary size and shape. Container is closed with tight lids. Usually 2:1 mass ratio of balls to the materials is advisable. If the container is more than half filled, the efficiency of milling is reduced. Heavy milling balls increase the impact energy on collision. Larger balls, used for milling, produce smaller grain size produce smaller grain size and larger defects in the particles. The process may add some impurities from balls. The container may be filled with air or inert gas. However this can be an additional source of impurity, if proper precaution to use high purity gases is not taken. A temperature rise in the range of 100^0C to 1100^0C is expected to take place during collision. Lower temperature favours amorphous particle formation. The gas like O_2, N_2 etc. can be the sources of impurities as constantly new, active surfaces are generated. Cryo-cooling (low temperature cooling) is used sometimes to dissipate the generated heat. The containers are rotated at high speed (a few hundred of rpm) around their own axis. Additionally they may rotate around some central axis and are therefore called as 'planetary ball mill [44]'.

When the containers are rotating around the central axis, the material is forced to walls and is pressed against the walls. But due to the motion of the container around their own axis, the material is forced to other region of the container. By controlling the speed of rotation of the central axis and container as well as duration of milling, it is possible to ground the material to fine powder whose size can be quite uniform [44].

2.3.5.Hysteresis Measurements of Multi-Layer Ceramic Capacitors Using a Sawyer-Tower Circuit:

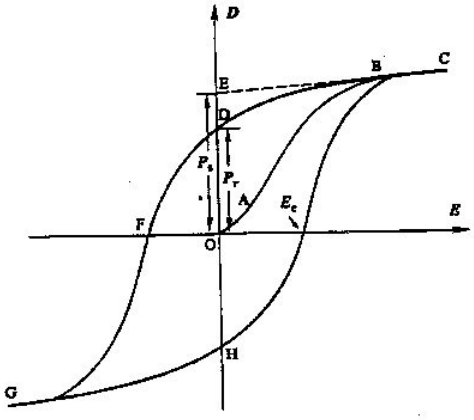

Fig 2.6 A Polarization vs. Electric Field (P-E) hysteresis loop for a typical ferroelectric crystal. [17]

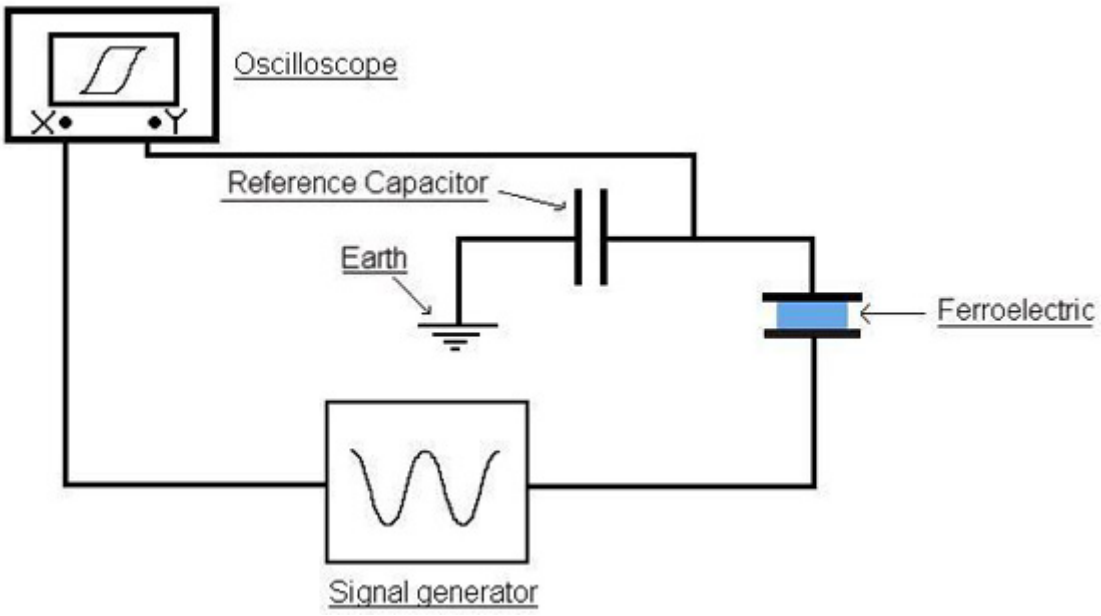

Fig 2.7: Block Diagram of Sawyer Tower Circuit

A ferroelectric hysteresis loop can be observed by means of a Sawyer Tower circuit. An alternating voltage V is imposed across a pair of electrodes on the surfaces of a ferroelectric crystal sample C_x placed on the horizontal plates of oscilloscopes; thus the

quantity plotted on the horizontal axis is proportional to the field across the crystal. A linear capacitor Co is therefore proportional to the polarization of the crystal Cx. This voltage is monitored by vertical plates of the oscilloscopes. If we first apply a small electric field is not large enough to switch any domain and the crystal will behave as a normal dielectric material (Para electric). This case corresponds to the segment OA of the curve as in fig2.6; As the electric field strength increases, a number of the negative domains (which have a polarization will increase rapidly (segment BC). This is a state of saturation in which the crystal is composed of just a single domain. As the field strength decreases, the polarization will generally decrease (at the point D in the figure2.6) but does not return back to zero. When the field is reduced to zero, some of the domain will remain aligned in the positive direction and the crystal will exhibit a remanent polarization Pr. The extra- polation of the linear segment BC of the curve back to the polarization axis (at the point E on the vertical axis in the fig2.6) represent the value of the spontaneous polarization Ps [16].

The remeant polarization Pr in a crystal cannot be removed until the applied field in the opposite direction reaches a certain value (at the point F in the fig2.6). The strength of the field required to reduce the polarization P to zero is called the 'coercive field strength' Ec. Further increase of the field in the negative direction will cause a complete alignment of the dipoles in this direction and the cycle can be completed by reversing the field direction once again. Thus the relation between P and E is represented by hysteresis (CDFGHC) as shown in figure2.6 [16].

3

RESULTS AND DISCUSSIONS

3.1. Optimization of milling duration:

It is well known that material's performances are dependent on their processing. Therefore, method of synthesis of ferroelectric materials played a significant role in determining the microstructural, electrical and optical properties of ferroelectric ceramics [33-35].

In the present work, SBT ferroelectric ceramics was synthesized by both the techniques i.e. Solid state reaction technique and Mechanical activation technique. Solid state reaction technique was used to synthesize the samples in the polycrystalline form and mechanical activation technique to synthesize the samples in the nanocrystalline form. Mechanical activation technique (high energy Ball milling) was used to synthesize various ferroelectric ceramics such as Lead Zirconate Titanate (PZT), Bismuth Titanate, Barium Titanate, Strontium Bismuth Tantalate etc. in its nano crystalline form.

The aim of the project is to optimize the milling duration for the synthesis of nano crystalline SBT ferroelectric ceramics. In the present work, samples of SBT were synthesized for three milling durations (5, 10, 20 hrs). Structural and electrical characterizations were carried out to optimize the best milling duration.

3.2. Structural characterization:

3.2.1. Solid State Reaction Technique:

Sintering Temperature: 1150^{o}C

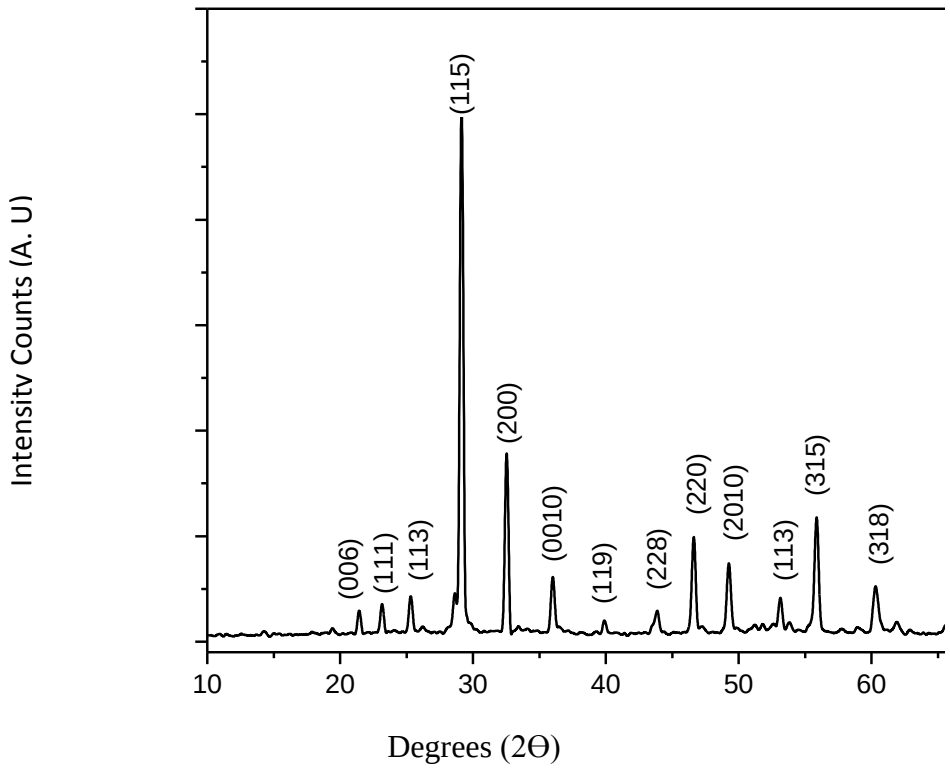

Fig 3.1 : XRD patterns of polycrystalline SBT sample

Fig. 3.1 shows the XRD patterns of synthesized polycrystalline SBT sample. The obtained XRD pattern is similar to the standard XRD pattern of SBT matched from JCPDS card file no.- 072-7073. Single phase layered pervoskite structure is formed without any secondary phase.

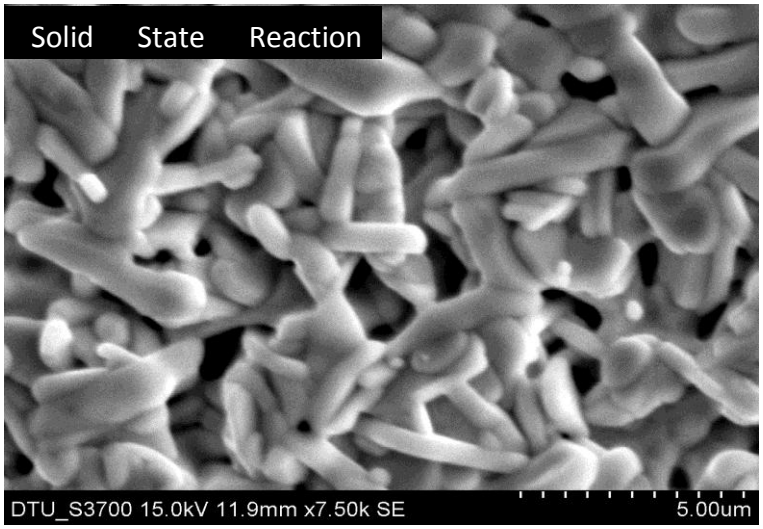

Fig 3.2: SEM image of the synthesized SBT sample

Fig 3.2 shows the SEM image of the synthesized SBT sample. It is observed that the grains are not homogeneously arranged. Porous and loosely packed morphology is observed. The approximate grain size (calculated from nearly 20 grain) is in the range of 3- 5 µm.

3.2.2. Mechanical Activation Technique.

Sintering Temperature: 1100 ^{o}C and 1150^{o}C

Milling Hours: 5, 10 and 20 hrs:

As discussed above, the starting oxides were taken in stoichiometric proportion and were milled in ball mill for various milling durations such as 5hrs, 10hrs and 20 hrs.

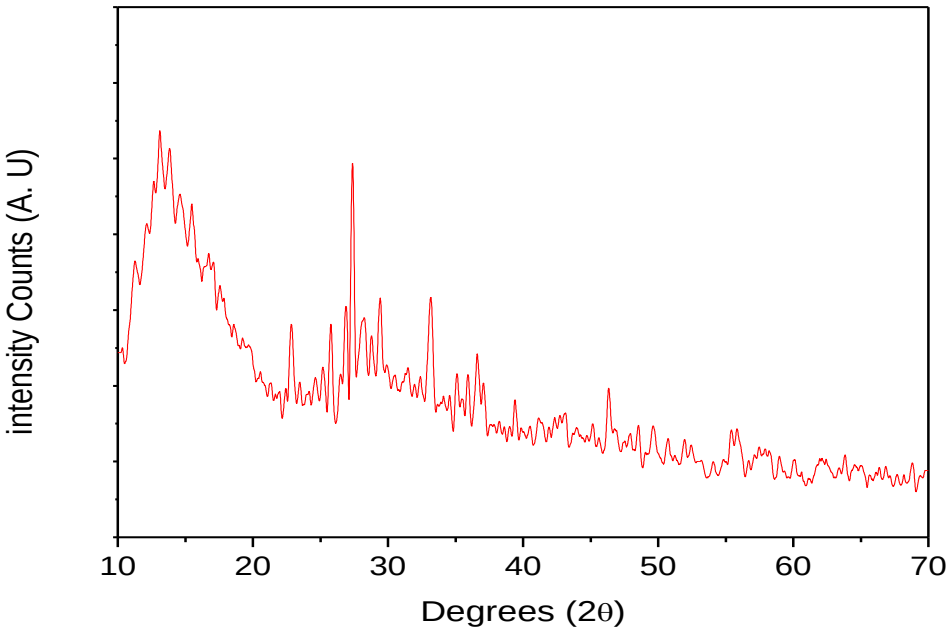

XRD pattern of 5 hrs milled powder

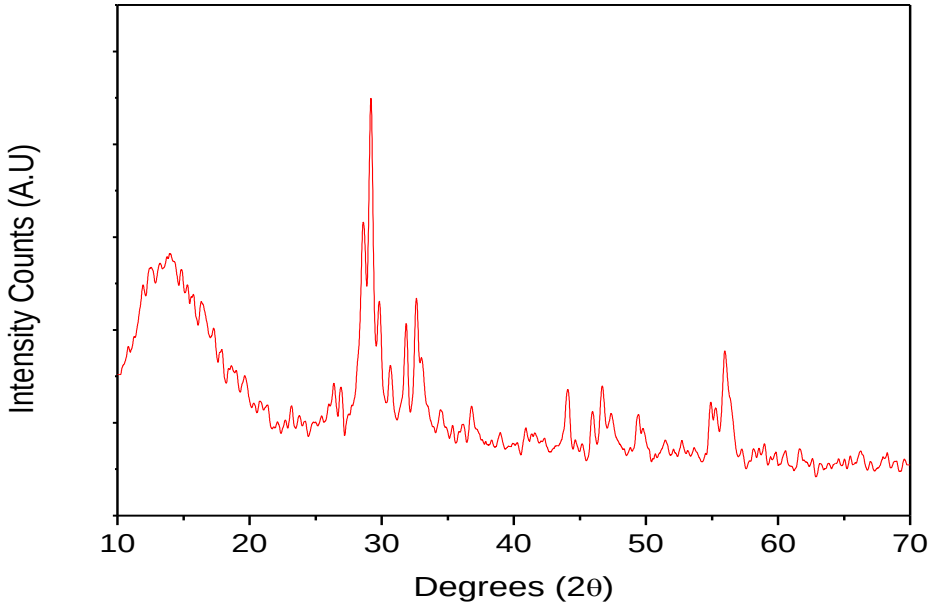

XRD pattern of 10hrs milled powder

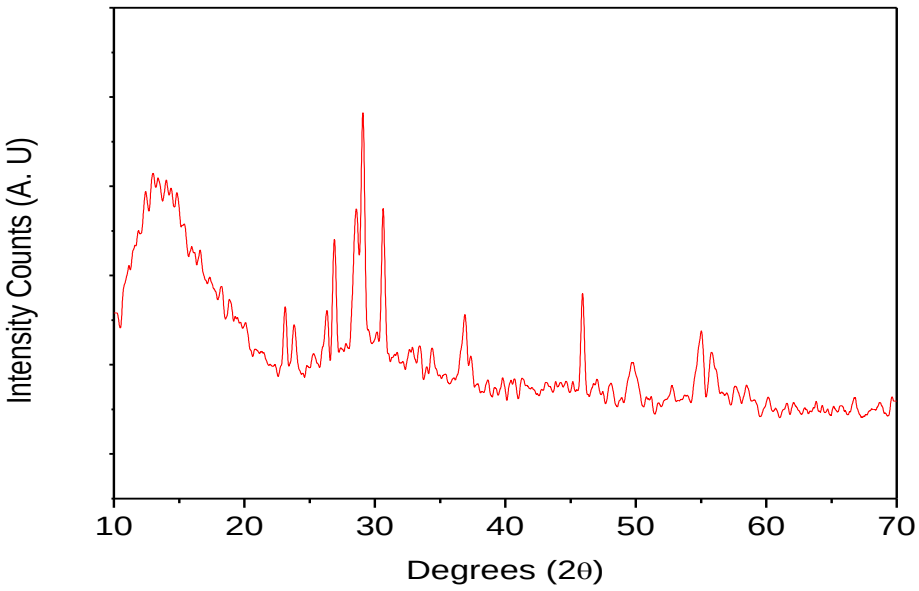

XRD pattern for 20hrs milled powder

Figure 3.3: XRD pattern of sample of SBT milled for 5hrs, 10hrs, 20 hrs

Fig. 3.3 compares the XRD pattern of the SBT powder milled for different duration of 5hrs, 10hrs and 20 hrs. It can be seen that phase development start from 5 hrs and improve with milling duration, because Particle size was decreasing as the milling duration increased so that grains arranged in more homogenously, and less porosity is observed..

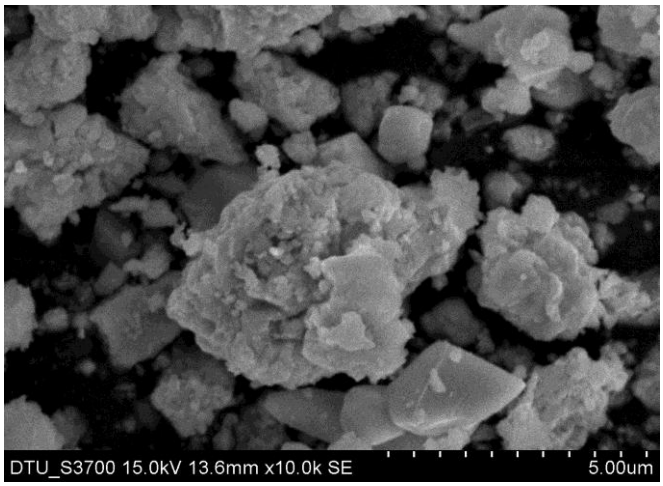

SEM Micrograph for 5 hrs milled powder

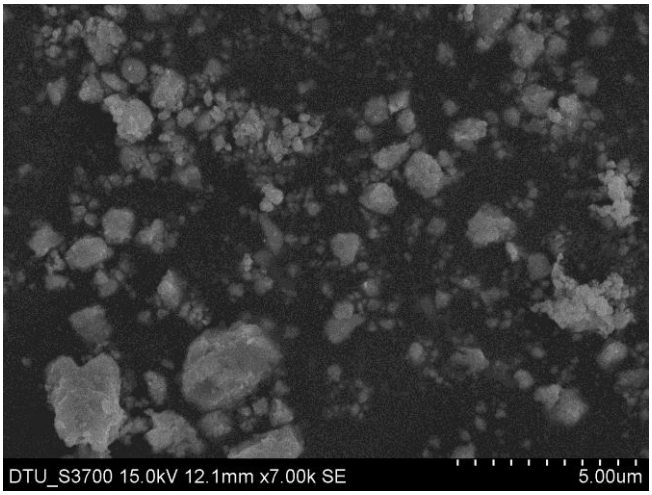

SEM Micrograph for 10hrs milled powder

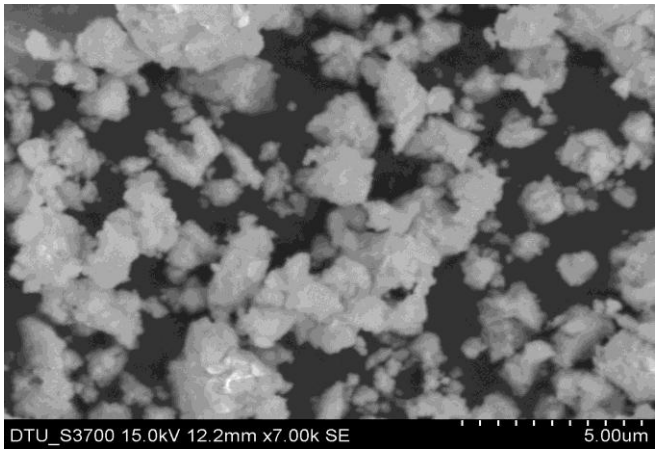

SEM micrograph for 20hrs milled powder

Figure3.4: SEM micrograph of sample of SBT milled for 5, 10 & 20 hrs

Fig. 3.4 show the SEM images of the specimen milled for different durations. The size of the particle can be seen to be getting reduced with increasing milling time. It is observed that sample milled for 20 hours shows slight agglomeration of particles. In Solid state reaction method Polycrystalline particle were formed, due to their rough grains, these powder require relatively high sintering temperature to obtain ferroelectric ceramic [33-35].

To reduce the sintering temperature, it is necessary to use the powder with small particle size. As the particle size decreases, surface to bulk atom ratio increases dramatically because more grain boundaries are formed. It can be easily understood that the number of surface atoms is quite large in nanoparticles and surface to bulk atom ratio goes on increasing with decreasing the particle size. Large surface related to large surface energy. This energy can be lowered by melting [44].

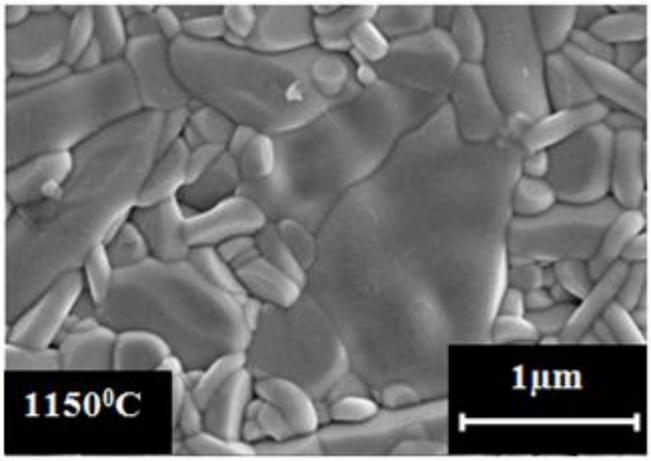

Fig 3.5: SEM micrographs of nanocrystalline SBT samples sintered at 1150^{0}C

Fig 3.5 shows the SEM micrographs of nanocrystalline SBT samples sintered at 1150^{0}C. After obtaining the milled powder, the pellets were formed for sintering. As discussed above, polycrystalline SBT sample was sintered at 1150^{0}C. Same procedure was applied to nanocrystalline SBT powder. It is observed that sample sintered at 1100^{0}C exhibit

homogeneous microstructure. The grains are densely packed with well defined grain boundaries. However, sample sintered at 1150^0C, exhibit poor morphology. As can be seen grains have started diffusing in to another. This is due to melting of sample at higher temperature because nanocrystalline powder sample was originally mechanically activated. Hence the sample was sintered at lower temperature i.e. 1100^0C, as can be observed in SEM micrograph.

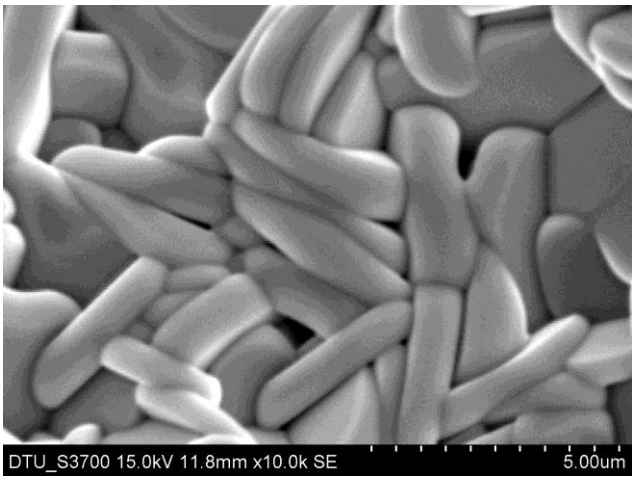

SEM micrograph of sintered (1100^0C) sample of 5 hrs

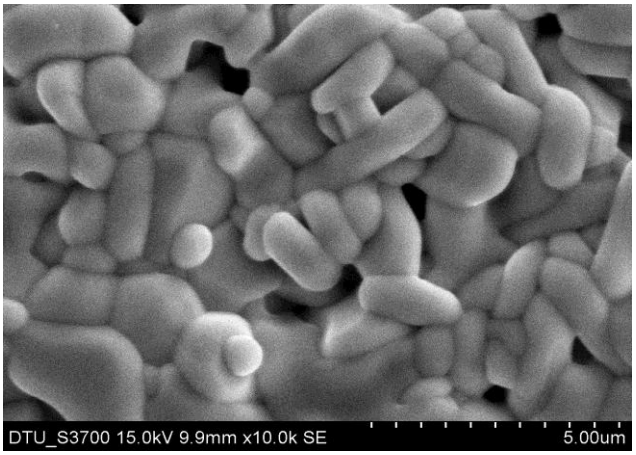

SEM micrograph of sintered (1100^0C) sample of 10 hrs

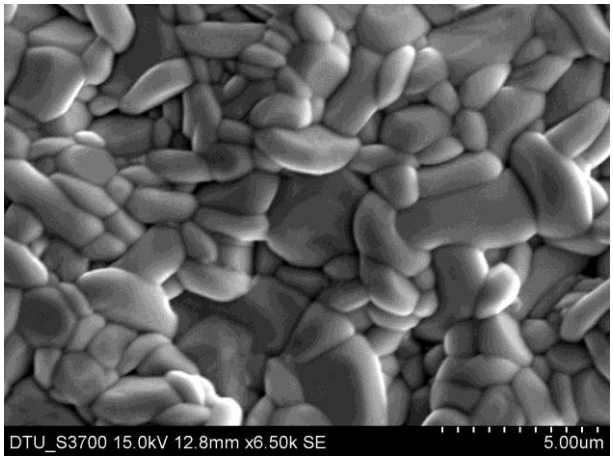

SEM Micrograph of sintered (1100^0C) of sample of 20 hrs

Fig 3.6: SEM micrographs of sintered samples (1100^0C) milled at different milling hrs.

Figure 3.6 shows the SEM micrographs of sintered samples (1100^0C) milled at different milling hrs. It is observed that the average grain size decreases as we increases the milling duration. The average grain size was found to be in the range of approximately 5-6µm, 900nm-1µm and 700-800 nm for sample milled at 5, 10 and 20 hrs respectively. Before palletization particle size was small, However after sintering increased particle size was observed due to melting, because within ball milling machine temperature raised in the range of 100^0C to 1100^0C [44] ,so that sample was already mechanically activated, and after sintering at 1100^0C some slight amount of melting may be happened due to this reason particle size was increased, after palletization and sintering. It was also observed that sample sintered by mechanical activation technique has dense and relatively porosity free microstructure as compared to sample synthesized by polycrystalline SBT samples (Fig.3.1). Due to the above discussed reason we did not perform the calcinations in mechanical activation technique because within the ball milling machine due to internal friction temperature raised up to near about to calcinations temperature, however calcinations was

required in solid state reaction technique, Further, it is also observed that 20 hrs milled sample has better microstructure.

3.3 Electrical Characterization:

3.3.1. Dielectric studies:

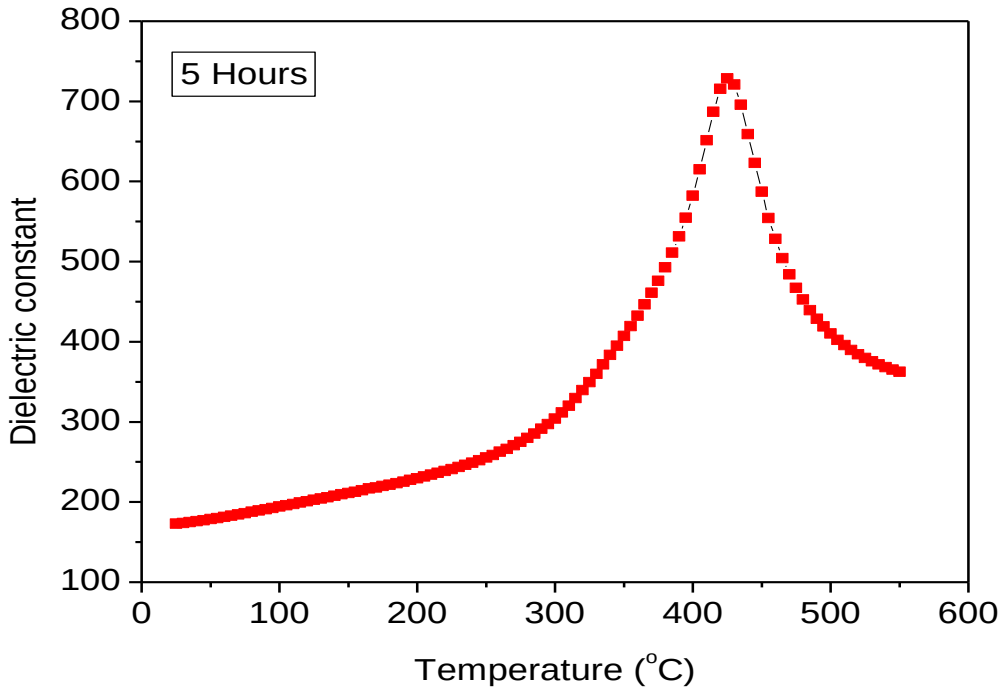

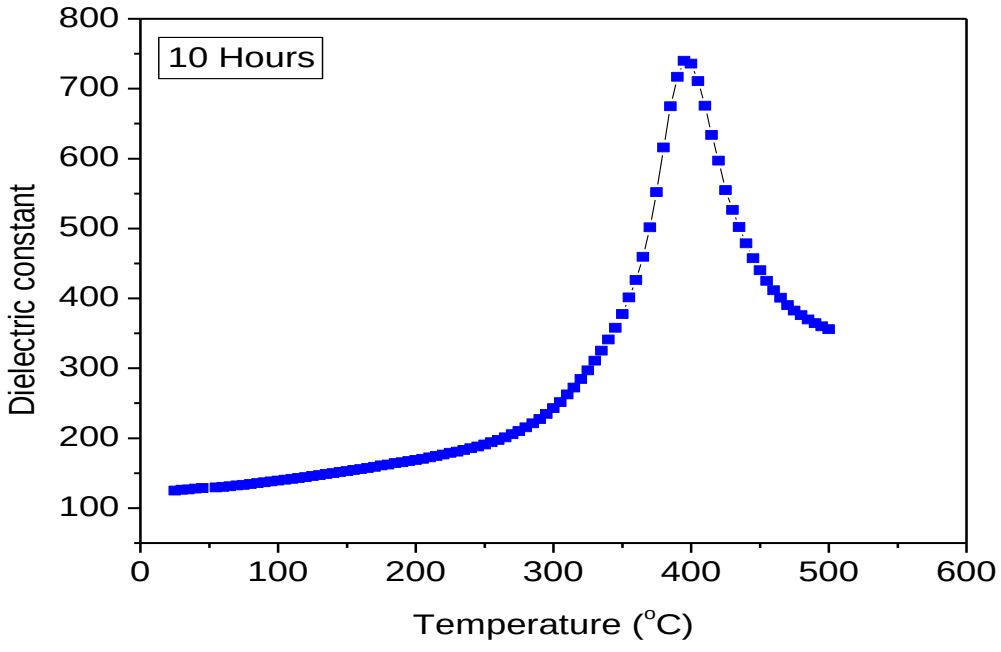

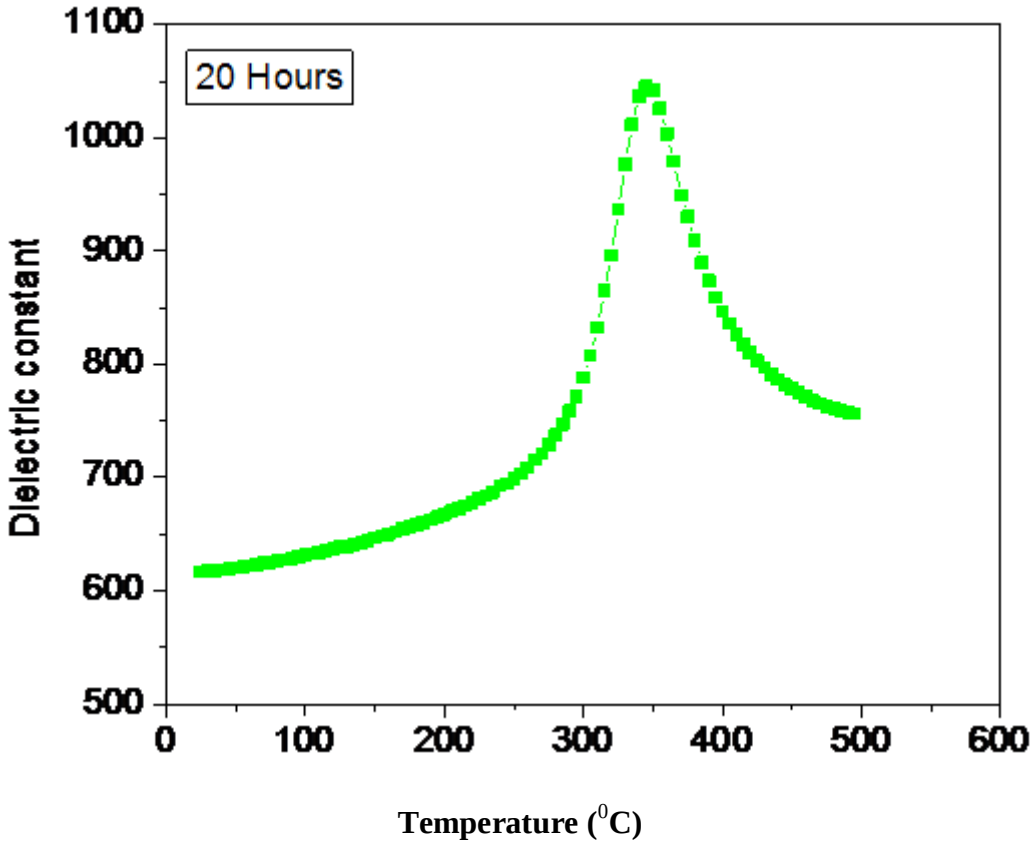

Fig 3.7: Temperature dependence of dielectric constant (ε_r) at 100 KHz

Figure 3.7 shows the temperature dependence of dielectric constant (ε_r) at 100 KHz measured for all milling duration. The compound show dielectric anomaly at a temperature called Curie temperature Tc indicating the occurrence of ferroelectric – paraelectric phase transition. It is observed that the value of dielectric constant increases with increase the milling duration and achieved maximum in the sample milled for 20 hrs. It is known that in the fine grained ferroelectric ceramic ε_r increase due to an increase in the residual stress [36-39], thus increase in ε_r value due to decrease in average grain size with milling time is observed. Also, as can be observed in figure 3.6, sample milled for 20 hrs milling duration exhibit porosity free microstructure as compared to lower milling duration samples. Thus the effect of space charges has been reduced because of less lattice vacancies, impurity centre [3]. Hence higher dielectric constant is observed in 20 hrs milled sample. Further, it is also observed that curie temperature is decreased, with increased in milling duration, because of

reduction in particle size. Curie temperature is dependent on the crystalline size, it decreases with reduction in crystalline size [39,40]. As particle size decreases, surface to bulk atom ratio increases [3], and more grain boundary are form which contain more grain boundary energy and large surface related to large surface energy, it required smaller amount of thermal energy [39,41,44].

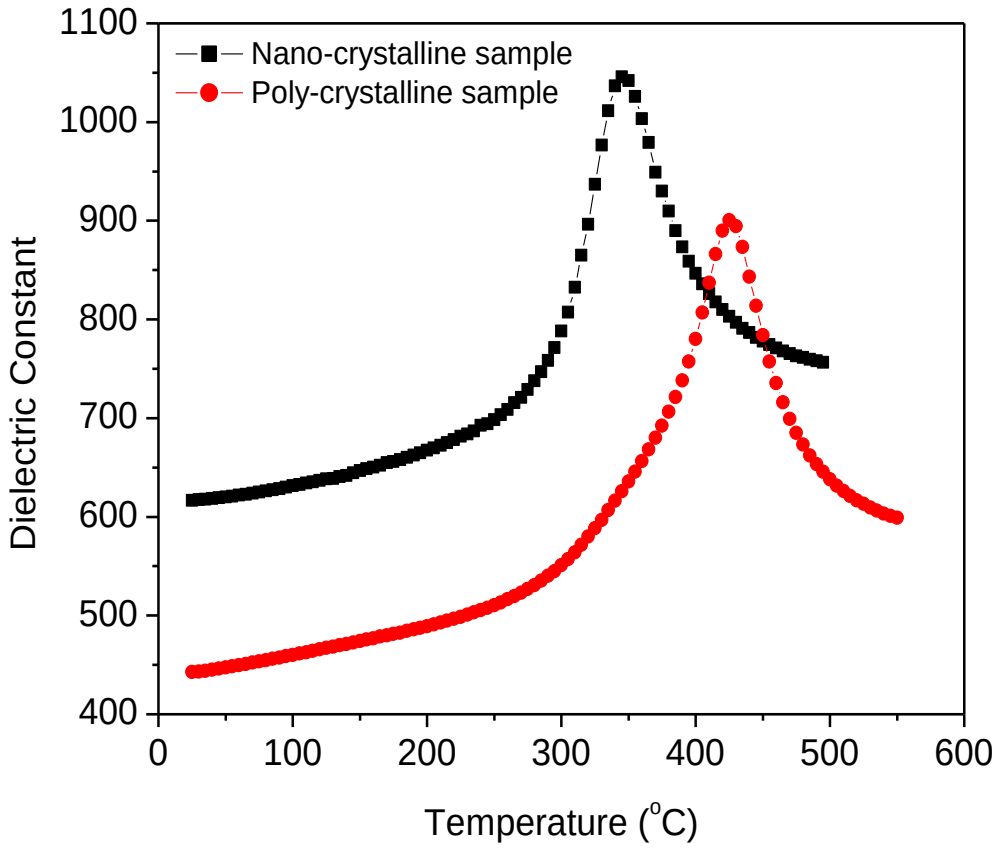

Fig: 3.8 Dielectric constant values as compared to polycrystalline SBT sample

Further in Fig 3.8 it is also observed that nanocrystalline sample milled for 20 hrs exhibit higher dielectric constant values as compared to polycrystalline SBT sample.

3.3.1.2. Dielectric loss:

Figure 3.10 shows the variation of dielectric loss as a function of temperature for all the studied samples.

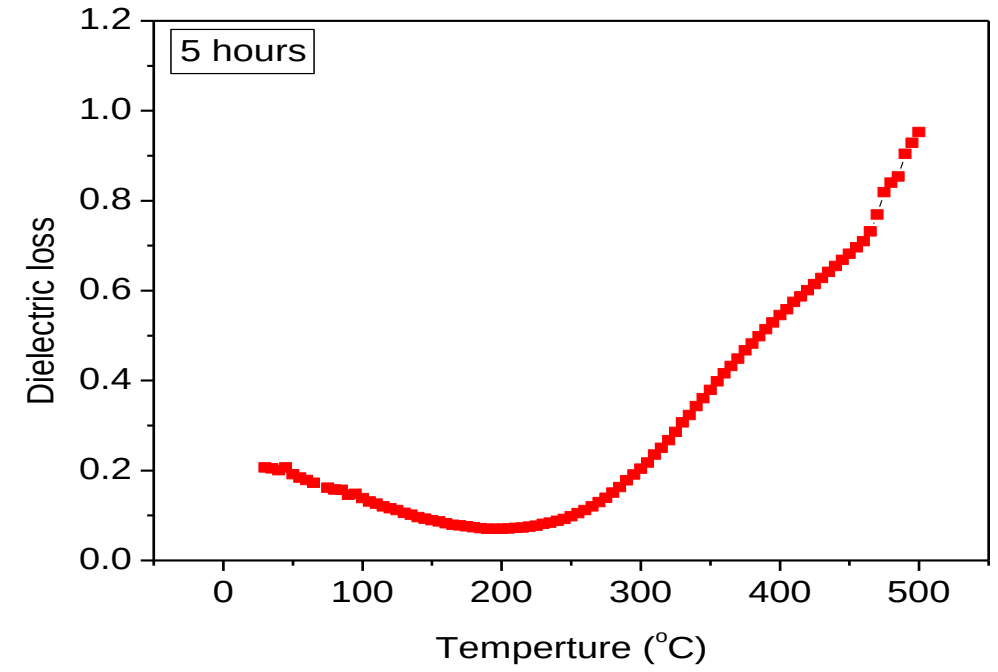

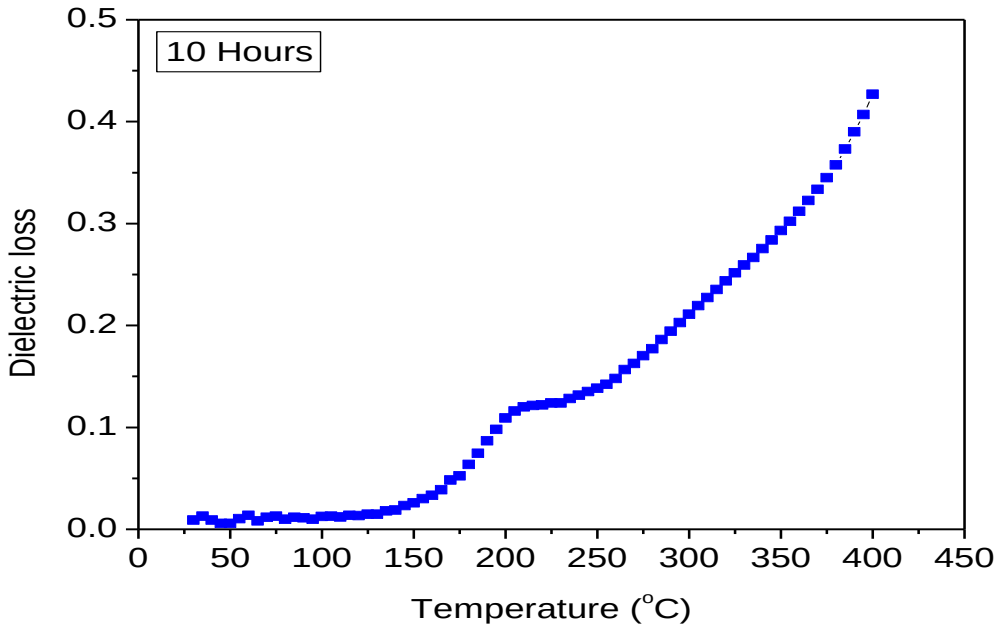

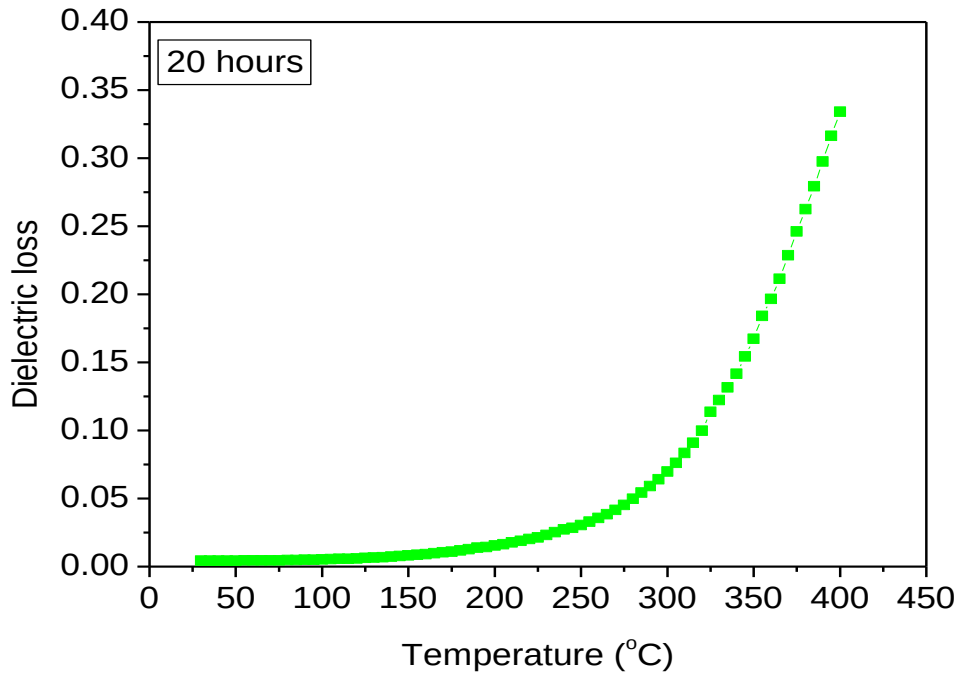

Fig 3.9: variation of dielectric loss as a function of temperature

It is observed that dielectric loss decreases with increasing milling duration and is minimum in the sample milled for 20 hrs. In all the samples it is observed that loss remains nearly constant in the lower temperature region and thereafter increases rapidly at higher temperature. Sample milled for 20 hrs did not show the increment in higher temperature region as compared to lower milling duration sample. The sharp increase of dielectric loss at high temperature region can be attributed to the increased mobility of space charges arising from defects or vacancies (oxygen vacancies) in the sample [39,42]. Also, the specimen milled for longer duration shows lower loss possibly because of improved and dense mirostructure having less porosity [39].

3.2.2. Ferroelectric studies:

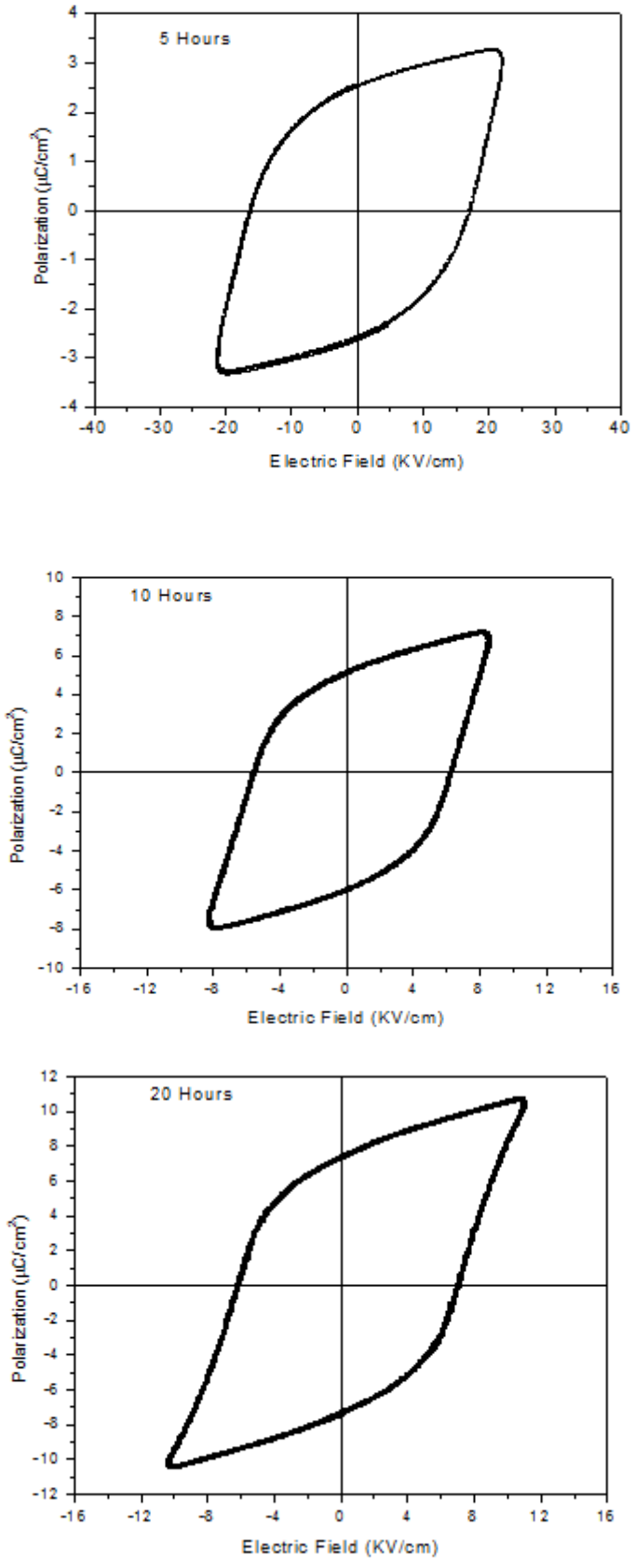

Fig 3.10: P-E Hysteresis loop for all the sample

Fig 3.11shows P-E hysteresis loops for sample milled for 5hrs, 10hrs, 20hrs.It is observed that all the samples exhibit ferroelectric nature. Further, remnant polarization (Pr) is observed to increase with increase in milling duration. Sample milled for highest milling duration (20 hrs) exhibit highest Pr values. This is possibly due to variation in application of electric field and smaller grains induce strong internal stress which would results in increased degree of dipole orientation [43]. As seen earlier, sample milled for 20 hrs has better microstructure. Hence it was observed that the breakdown voltage of the sample was higher as compared to lower milling hrs samples. Thus better switching of domains resulted in higher saturation and polarization values. Further, sample milled for 5hrs and 10hrs has poor microstructure. Therefore space charges are trapped in the vacant space resulting pinning of domain walls. Thus lower remnant polarization value is observed [16].

4

CONCLUSIONS

From the above experimental result and discussion it is concluded that synthesis of nanocrystalline SBT ferroelectric ceramics has been done successfully using mechanical activation technique and synthesis of polycrystalline SBT ferroelectric ceramic done successfully using solid state reaction method. XRD, SEM was used to determine the structure of synthesized samples. In solid state reaction method the size of the polycrystalline SBT particle was found in range of 3-5µm. In mechanical activation method, the particle size has been observed to decrease as we increased the milling duration successively from 5hrs to 20hrs and particle size was observed for 20 hrs sintered pellet 700 – 800nm; it is also observed that agglomeration was started, From SEM micrograph of 20 hrs milled powder.

Electrical studies of both types of samples were also performed. In, electrical studies, such as the values of dielectric constant, the value of dielectric loss and P-E hysteresis loop confirms that enhanced properties are observed for sample milled for higher milling duration. It is observed that the value of dielectric constant increases with increase the milling duration and achieved maximum in the sample milled for 20 hrs. It is also observed that dielectric loss decreased due to increased milling duration, dielectric loss was minimum for 20hrs milled powder. From P-E hysteresis loop analysis it is also observed that remnant polarization (Pr) increased with increasing in milling duration. Sample milled for highest milling duration (20 hrs) shown highest Pr values 7.8µc/cm^2 in comparison to 5 hrs milled sample. A comparison of Dielectric properties of nanocrystalline sample and polycrystalline sample was also done and it was found that dielectric constant of 20hrs milled powder was higher than polycrystalline sample. So finally we can say that nanocrystalline SBT sample has better structural and electrical property in comparison to polycrystalline sample.

References

[1] J.Valasek, Phys. Rev., 17,475 (1921).

[2] Serguei Brazovskii, Natasha Kirova ," Ferroelectricity in synthetic metals: Reality and hypotheses", Synthetic Metals 2205–2207,159 (2009) .

[3] S.P.Seth, Electrical Engineering Materials, (Dhanpat Rai Publication,3rd edition, 2003).

[4] Desu SB, Vijay DP. Mater Sci Eng 1995;B 32:83–8.

[5] Indrani Coondoo , A.K. Jha, Materials Letters 63 (2009) 48–50 .

[6] http://www.azom.com/article.aspx?ArticleID=3593

[7]R.C. Buchanan, Ceramic Materials for Electronics: Processing, Properties and Application(Marcel Dekker Inc. N.Y.).

[8] S.O.Kasap, Principle of Electronic Materials and Devices, 2nd edition (Tata McGraw – Hill Inc., N.Y., 2002).

[9] M.Deri, Ferroelectric Ceramics(Akademiai Kiado, Budapest,1966).

[10] J.F. Scott (2000). Ferroelectric Memories. Springer.

[11]A.Von .Hipple, Rev. Modern Phys., 22, 221, (1970).

[12] R.E. Netteleton, Ferroelectrics, 1,221,(1970).

[13] garfield.chem.elte.hu/turanyi/oktatas/Pharmacy.../02ElProp2.doc.

[14] http://en.wikipedia.org/wiki/Relative_permittivity.

[15] A.J. Dekker, Solid State Physics(Macmillan,NY,1991).

[16] Y.H. Xu, Ferroelectric Material (Elsevier Science Publishers, Amsterdam, 1991).

[17] J. F. Nye, Physical Properties of Crystals (Clarendon Press, Oxford, 1990).

[18] W.J.Merz,Phys.Rev., 91, 513(1953).

[19]Y. Xu, Ferroelectric Materials and their Applications (North Holland, Amsterdam, 1991).

[20] A. Baudrant, H. Vial, and J. daval, J. Cryst. Growth, **43**, 197 (1978).

[21] S. Miyazawa and N. Uchida, Opt. and Quantam Electronics, **7**, 451 (1975).

[22] C. E. Land, J. Am. Ceram Soc., **72**, 2059 (1989).

[23] http://www.scitec.uk.com/infrared_detectors/faq.php.

[24] L. E. Cross, Ferroelectric Ceramics-Tutorial Reviews, Theory, Processing and Applications, N. Setter, and E. L. Colla, ed., 1 (Birkhauser Verlag, Basel, 1993)Hard PZT.

[25] J. Nuffer, D.C. Lupascu, J. R¨odel, Stability of pinning centers in fatigued lead–zirconate–titanate, Appl. Phys. Lett. 80 (2002) 1049–1051.

[26] Hyeong-Ho Park , Hyung-Ho Park , Tae Song Kim, Ross H. Hill , Sensors and Actuators B 130 (2008) 696–700.

[27] B.Jaffe, W.R. Cook & H.Jaffe, Pizeoelectric Ceramic(Academic,London,1971).

[28] A.D.Rae, J.G.Thomson & R.L.Wither, Acta. Crysallogr .Sect.,B48,418,(1992).

[29] Christian Erich Zybill , Mahmoud Abdel-Hafiez ,Sami Allam , Tharwat El Sherbini, Progress in Solid State Chemistry 35 (2007) 469e480

[30] Paz de Araujo CA, Scott JF. Science 1989;246:1400–4.

[31] Indrani Coondoo, A.K. Jha , S.K. Agarwal , Journal of the European Ceramic Society 27 (2007) 253–260.

[32] Irie, H., Miyayama, M. and Kudo, T. , J. Appl. Phys., 2001, **90**, 4089–4094.

[33] Kiezer K, Janssen EH and Burggraaf AJ. Influence of particle size and structure of ZrO_2 on microstructure development and dielectric constant of $Pb(Zr_{0.5}Ti_{0.5})O_3$. Mater Res Bull 533-44; 8: (1973).

[34]Yamamoto T. Optimum preparation methods for piezoelectric ceramics and their evalution. Am Ceram Soc Bull;: 978-85, 71 (1992).

[35]Arlt G. The influence of microstructure on the properties of ferroelectric ceramics. Ferroelectrics; 217-27,104: (1990)

[36]Buessem WR, Cross LE and Goswami AK. Phenomenological theory of high permittivity in fine-grained barium titanate. J Am Ceram Soc 33-6, 49 [1](1966);

[37]Arlt G, Henning D and With G de. Dielectric properties of fine-grained Barium Titanate Ceramics. J Appl Phys; 1619-25, 58 [4];(1985).

[38]Uchino K, Sadanaga E and Hirose T. Dependence of the crystal structure on particle size in Barium Titanate. J Am Ceram Soc; 1555-8,72 [8],(1989).

[39] Sugandha, A.K.Jha, Material Characterization, 65 (2012) 126- 132.

[40] Parashar SKS, Choudhary RNP, Murthy BS. J Appl Phys 2003;94(9):6091–6.

[41] Callister WD. Material Science and Engineering: An Inroduction', Wiley, India,

(2006).

[42] Ganguly P and Jha AK. Enhancement of dielectric properties by optimization of

sintering condition in tungsten–bronze structured Ba5SmTi3Nb7O30 ferroelectric

12 ceramics. J Electroceram; 257-62,22: (2009).

[43]P.Ganguly & A.K. Jha, J.Am. Cream. Soc.,1-6,34,2011.

[44] Sulbha Kulkarni, Nano Technology: Principles and Practices, Capital Publishing,Kolkata.

[45] LCR Meter , Wikipedia

[46] mrl.upesh.edu.pk/facilities/lcr_meter